Review

An Overview of Selected Material Properties in Finite-Element Modeling of the Human Femur

Pourya Bazyar [1,*], Andreas Baumgart [2], Holm Altenbatch[3] and Anna Usbeck [4]

1. Department of Mechanical Engineering and Production Management, University of Applied Science,Germany; pourya.bazyar@haw-hamburg.de
2. Department of Mechanical Engineering and Production Management, University of Applied Science, Germany; a.baumgart@haw-hamburg.de
3. Institute of Mechanics, Faculty of Mechanical Engineering, Otto-von-Guericke University Magdeburg, Magdeburg, Germany; holm.altenbach@ovgu.de
4. Department of Mechanical Engineering and Production Management, University of Applied Science, Germany; annakerstin.usbeck@haw-hamburg.de

* Correspondence: pourya.bazyar@haw-hamburg.de; Tel.: +4915207101359

Abstract: specific finite detail modeling of the human body gives a capability primary enhancement to the prediction of damage risk all through automobile impacts. currently, car crash protection countermeasure improvement is based on an aggregate of testing with installed anthropomorphic check devices (i.e., ATD or dummy) and a mixture of multibody (dummy) and finite element detail (vehicle) modeling. If an incredibly easy finite element detail version can be advanced to capture extra statistics beyond the abilities of the multi-body structures, it might allow advanced countermeasure improvement thru more targeted prediction of overall performance. Numerous research have been done on finite element analysis of broken femurs. However, there are two missing pieces of information: 1- choosing the right material properties and 2- designing a precise model including the inner structure of the bone. In this research, most of the chosen material properties for femur bone will be discussed and evaluated.

Keywords: femur; material; isotropic; anisotropic; orthotropic

1. Introduction

Finite Element Analysis has a large number of usages in medical, agricultural, and mechanical products (Bazyar, et al., 2020; Bazyar & Baumgart, 2021). Finite-element modeling of the human femur, like most biological structures (Jacrot, 1976), has an inherent trouble in that building a material model capable of describing the 2 complex bone tissues Amini, (et al., 2012), cortical and cancellous, is extremely worrying. Consequently, the development of any such finite-element model is a whole lot of extra time-ingesting and the level of expertise in non-linear material continuum mechanics required to enhance correct fabric model descriptions is a good deal better. This caveat necessitates the significance of investigating whether this excessive degree of material model complexity (in particular in the anisotropic description) is essential. The human femur has, via numerous investigations, been physically examined (human cadaver complete bones) yielding knowledge on obvious complete-bone residences (e.g., whole-bone elastic bending stiffness (Mather, 1967; Yamada, 1970; Martens,et al, 1986; Keller, et al., 1990, Zani, et al., 2015; Arun & Jadhav, 2016). It has also been digitized and modeled in lots of distinct finite element applications both at the tissue level and at the complete-bone macroscopic level (Schuster, et al., 2000; Pellettiere, 1999; Wirtz, et al, 2000; Ciarelli, et al., 1991; Osterhoff, et al., 2016). lots of designs have additionally been achieved to ascertain the femur bone tissue materials' (cortical and cancellous) linear and non-linear material properties by way of methods starting from mechanical and acoustic testing to more theoretical way (Reilly & Burnstein, 1974; Choi, et al., 1990; Ciarelli, et al., 1990; Ciarelli, et al., 1991; Keaveny, et al., 1994;

Preprints (www.preprints.org) | NOT PEER-REVIEWED | Posted: 27 December 2022 doi:10.20944/preprints202212.0503.v1

Bayraktar, et al., 2004; Augat, et al., 1998; Zysset, 2003; Cristofolini, et al., 1996; Kabel, et al., 1999; Morgan, et al., 2003; Morgan and Keaveny, 2001). The more accurate FE design of the femur entire bone, or separately, the bone tissues, encompass fabric design that describes a few grades of fabric anisotropy, or specific directional conduct (Pellettiere, 1999), in addition to pressure fee dependence. In terms of Fig.1, there are a colossal number of sections inside of the bone that contains marrow, trabeculae, Haversian canals, etc. (Yeni, et al. 1997). Most of the researchers were done FE analysis on the fractured femur with STL file of human femur fixed with different types of implants (DHS, CS, etc.) (Falcinelli & Whyne, 2020; Chethan, et al., 2019; Schileo, et al., 2020, Zhang, et al., 2022; Tucker, 2019; Mobasseri, 2022; Kalaiyarasan, 2020). Therefore, researchers are unable to design a model of the human with design three. Some of them designed a simplified model of the human femur and waive other parts of the femur (Bazyar, et al., 2022). In this research 3 sections of the bone (cortical, trabeculae, and marrow) with three types of material (Isotropic, Anisotropic, and Orthotropic) were discussed, and explained the approach of defining them in Ansys. In the next parts, different types of material will be illustrated step by step.

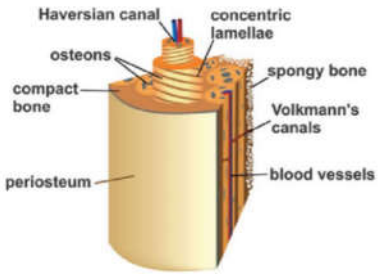

Figure 1. Inner structure of the bone.

1.1. Types of material properties:

This section demonstrates the major types of material properties (Isotropic, Anisotropic, and Orthotropic), which were used in FE analysis of the human femur, will be introduced precisely.

1.1.1. Isotropic materials

Isotropic materials have similar physical and mechanical properties in all directions. It shows that the identical strength, stress, strain, young's modulus, and hardness will be evaluated when a selected load is carried out at any point inside the x, y, or z-axis, isotropic materials. Additionally, isotropic material does not have a dependency on the direction of light travels. It has just a deflection index. The deflection index is the ratio of light speed in a vacuum to the phase rate in a material through which light moves. So, light speed in isotopic is not impacted via the varying direction of irradiation. The elastic Young's modulus (E) and Poisson's ratio (v) are the main properties that were used for femur analysis with isotropic material. They show material stiffness and the ratio of lateral strain to axial strain respectively (Czarnecki, 2015).

1.1.2. Anisotropic materials

Anisotropic materials, additionally mentioned as "triclinic" materials, depend on directions that are made from the unsymmetrical crystalline structure. In other words, there is a relation between the mechanical behavior of anisotropic materials and the orientation of the material's body. When the same load is applied to various axes, each surface responds differently. This suggests that measurements of a particular mechanical or thermal property taken along the x-axis will be different from measurements taken along the y-axis or z-axis. Additionally, regarding reference axes, there are differences in the concentration and distribution of atoms. Therefore, the measurements also change as the axis does. There are five independent properties an anisotropic material including two

Preprints (www.preprints.org) | NOT PEER-REVIEWED | Posted: 27 December 2022 doi:10.20944/preprints202212.0503.v1

Young's moduli, E1 (principal modulus) and E3 (or E2, modulus in the transverse plane), two shear moduli, G12 (or G13) and G23. and one Poisson ratio, v. (Ahn, 2002).

1.1.3. Orthotropic Materials

If a material exhibits distinct and independent mechanical or thermal characteristics in three mutually perpendicular directions, it is said to be orthotropic. Wood, many crystals, and rolling metals are a few examples of orthotropic materials. For instance, the longitudinal, radial, and tangential directions are used to explain the mechanical characteristics of wood at a place. The radial axis (2) is normal, while the longitudinal axis (1) is parallel to the direction of the grain (fiber); the radial axis (2) is normal to the growth rings, and the tangential axis (3) is tangent to the growth rings (fig. 1). there are nine independent material properties that entail Young's moduli in three directions (E1, E2. E3), a trio of shear moduli (G12. G13. G23), and three Poisson's ratios (v12, v13, v23) (Peng, et al., 2006). These are limited, 1n a thermodynamically constant material, with:

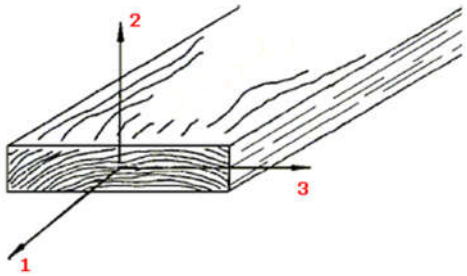

Figure 2. Kind of orthotropic material.

$E_1, E_2, E_3, G_{12}, G_{23}, G_{31} > 0$ (1)

$C_{11}, C_n, C_{33}, C_{44}, C_{55}, C_{66} > 0$ (2)

$(1- U_{23} U_{32}). (1- U_{13} U_{31}). (1-u12\ U21) > 0$ (3)

$1-(U_{12} U_{21}) - (U_{23} U_{32}) - (U_{31} U_{13})-2(U_{21} U_{32} U_{13}) > 0$ (4)

Also, by symmetry,

$$v_{ji} = v_{ij} \frac{E_{jj}}{E_{ii}} \quad (5)$$

Equations (2) and (5) create the conditions shown below.

$$|v_{21}| \le \left[\frac{E_{22}}{E_{11}}\right]^{\frac{1}{2}}, \quad |v_{12}| \le \left[\frac{E_{11}}{E_{22}}\right]^{\frac{1}{2}}, \quad |v_{32}| \le \left[\frac{E_{33}}{E_{22}}\right]^{\frac{1}{2}}$$

(10)

$$|v_{23}| \le \left[\frac{E_{22}}{E_{33}}\right]^{\frac{1}{2}}, \quad |v_{31}| \le \left[\frac{E_{33}}{E_{11}}\right]^{\frac{1}{2}}, \quad |v_{13}| \le \left[\frac{E_{11}}{E_{33}}\right]^{\frac{1}{2}}$$

With the selection of the material parameters used in this investigation, equation (1) is trivially satisfied. Both trabeculae and cortical bone's material qualities meet the requirements of equations (3), (4), and (5).

Preprints (www.preprints.org) | NOT PEER-REVIEWED | Posted: 27 December 2022 doi:10.20944/preprints202212.0503.v1

1.2. Physical and mechanical properties of the human femur

Data from mechanical tensile tests were used where they were pertinent to the circumstances of this study. Not every range given in the literature applies to all of the material constants utilized in this investigation. This difference is to be expected given the many factors, such as age, pathology, and sample size. To give the material models' average properties, tabulated tissue response data and average values from several investigations are employed whenever practical. The specific material inputs selected for each material model are shown in this section. For the sake of model simplicity, the separate bone tissues are also given a uniform apparent density throughout the femur of 1.9 g/cm^3 for cortical tissue and 0.4 g/cm^3 for trabecular tissue. This is in addition to the mechanical properties indicated.

1.2.1. Material properties for trabeculae

Elected orthotropic material qualities are listed in Table 1. The following criteria guided the selection of these:

1. All orthogonal moduli are comparable to values published in (Wirtz, et al., 2000) and (Morgan, et al., 2003) and fall within the generally accepted range of 0-4.74 GPa (Morgan and Keaveny, 2001).
2. For cancellous bone tissue, the ratios of the directional Young's moduli exhibit a relationship similar to that reported in (Augat, 1998), where E_1/E_2 and E_1/E_3 are equal to approximately 2 (here, equal to 1.4 and 2.0, respectively), and E_3/E_2 is equal to approximately 0.6 (here, 0.07).
3. The typical Young's modulus is 1.0 GPa, which is in accordance with what has been documented in the literature.

The selected isotropic and anisotropic material properties for cancellous bone are shown in Tables 2 and 3. Notably, the shear moduli in planes 1-3 and 1-2 were averaged to 399 MPa for the transversely isotropic material model, whereas the moduli in the 2 and 3 directions were 822 MPa on average. The average Young's modulus and average Poisson's ratio for the isotropic model are 1.0 GPa and 0.3, respectively.

The inputs for the isotropic piecewise linear plasticity material model of cancellous bone are displayed in Table 4. According to (Bayraktar, et al., 2004), the tangent modulus is set at 5% of the elastic modulus. The yield stress is the average of the values for the greater trochanter and femoral neck described in (Morgan & Keaveny, 2001), which is roughly 3 MPa and 12 MPa, respectively.

Table 1. Trabeculae as an orthotropic material.

Young's Moduli (MPa)	Shear Moduli (MPa)	Poisson's Ratios
$E_1 = 1352$	$G_{12} = 292$	$V_{12} = 0.30$
$E_2 = 968$	$G_{23} = 370$	$V_{23} = 0.30$
$E_3 = 676$	$G_{13} = 505$	$V_{13} = 0.30$

Table 2. Trabeculae as an anisotropic material.

Young's Moduli (MPa)	Shear Moduli (MPa)	Poisson's Ratios
$E_1 = 1352$	$G_{12} = 399$	$V_{12} = 0.30$
$E_2 = 822$	$G_{23} = 370$	$V_{23} = 0.30$
$E_3 = 822$	$G_{13} = 399$	$V_{13} = 0.30$

Table 3. Trabeculae as an isotropic material.

Young's Moduli (GPA)	Poisson's Ratios
$E_1 = 1$	$V_{12} = 0.30$

Preprints (www.preprints.org) | NOT PEER-REVIEWED | Posted: 27 December 2022 doi:10.20944/preprints202212.0503.v1

Table 4. Trabeculae as a nonlinear isotopic model.

Elastic Modulus (MPa)	Tangent Modulus (MPa)	Poisson's Ratios	Yield Stress (MPa)
E= 1000	E_{tan}= 1000	0.3	7.5

1.2.2. Material properties for cortical

One of the few researchers that has looked into the directional moduli of cortical bone is Reilly & Burnstein (Reilly & Burnstein, 1974). The results are mentioned below:

E_1 = 8.69 GPa (longitudinal), E_2 = 4.19 GPa (transverse), E_3 = 3.76 GPa (radial).

The following ratios, presented as approximate percentages, can be extracted from the data, despite the fact that this E_1 is substantially lower than that of the majority of other studies: E_2/E_1 = 48%, E_3/E_2 = 90%, and E_3/E_1 = 43%. The longitudinal tensile and bending moduli for wet human cortical bone specimens, principally from the femur, are listed in detail in Table 5 (Choi, et al., 1990). As can be observed, the average longitudinal Young's modulus throughout these experiments is 16.0 GPa. Using the aforementioned percentages, E_2 and E3 are equivalent to roughly 6.8 GPa and 6.3 GPa, respectively, with E1 equal to 16.0 GPa. Shear moduli are found in Schuster (Schuster, et al., 2000) and are comparable to the 3.36 GPa reported as the average shear modulus by Reilly & Burnstein (Reilly & Burnstein, 1974). In another research, Mirzaali, et al. (Mirzaali, et al., 2016) evaluated the physical and mechanical properties of cortical in different cases. It was written that the axial hardness modulus for Osteonal, Interstitial, and pooled bone are 408±69, 503±56, and 455±78 respectively. Therefore, transverse hardness modulus for female, male and pooled bone are 367±91, 428±75, and 395±89 respectively. In uniaxial tests, the Modulus are 18.16 ± 1.88 and 18.97 ± 1.84 under uniaxial tension and compression respectively. The Reilly & Burnstein (Reilly & Burnstein, 1974) Poisson's ratios for cortical tissue are 0.62 for "radial specimens" and 0.40 for "longitudinal specimens." Since Poisson ratios greater than 0.5 are not permitted in the infinitesimal theory, these values led to problems in the constitutive equations used for the orthotropic material model. As a result, the ratios were reduced while maintaining their relative magnitudes. The radial and longitudinal Poisson's ratios are scaled to 0.45 and 0.30, respectively. These are comparable to the average Poisson's ratio for femoral cortical bone tissue reported by Katsamanis & Raftopoulos (Katsamanis & Raftopoulos,1990) of 0.36. The transverse direction Poisson's ratio in this study is also calculated using the Poisson's ratio for the radially harvested specimen (set to 0.3). Table 6 lists the final nine elastic material constants used for the orthotropic cortical bone. The orthotropic material model description with E_2 = E_3 = 6.30 GPa and G_{12} = G_{13} = 3.30 is all that is required to describe the transversely isotropic material model for cortical tissue, as illustrated in Table 7. Table 8 displays the isotropic material model description for cortical tissue. The material constants for the isotropic piecewise-linear-plasticity material model of cortical bone are displayed in Table 9. The yield stress is the average of the values for specimens tested in tension by Reilly & Burnstein (Reilly & Burnstein, 1974), and the elastic modulus and Poisson's ratio are the same used for the elastic, isotropic model. The tangent modulus is 5% of the elastic modulus (Bayraktar, et al., 2004).

Table 5. Cortical as an orthotropic material.

Young's Moduli (GPa)	Shear Moduli (GPa)	Poisson's Ratios
E_1 = 16	G_{12} = 3.2	V_{12} = 0.30
E_2 = 6.88	G_{23} = 3.6	V_{23} = 0.45
E_3 = 6.30	G_{13} = 3.3	V_{13} = 0.30

Preprints (www.preprints.org) | NOT PEER-REVIEWED | Posted: 27 December 2022 doi:10.20944/preprints202212.0503.v1

Table 6. Cortical as an anisotropic material.

Young's Moduli (GPa)	Shear Moduli (GPa)	Poisson's Ratios
$E_1 = 16$	$G_{12} = 3.3$	$V_{12} = 0.30$
$E_2 = 6.30$	$G_{23} = 3.6$	$V_{23} = 0.45$
$E_3 = 6.30$	$G_{13} = 3.3$	$V_{13} = 0.30$

Table 7. Cortical as an isotropic material.

Young's Moduli (GPa)	Poisson's Ratios
$E_1 = 16$	$V_{12} = 0.36$

Table 8. Cortical as a nonlinear isotopic model.

Elastic Modulus (GPa)	Tangent Modulus (MPa)	Poisson's Ratios	Yield Stress (MPa)
E= 16	E_{tan}= 800	0.36	108

1.2.3. Material properties for Morrow

In comparison to past investigations, our data on bone marrow mechanics are both substantially stiffer and covers a wider range of values. However, as was already mentioned, other research have used homogenized tissue samples, so it is difficult to compare the reported viscosities, which range from 44.6 to 142 mPas, with our data, which range from 100 to 500 Pa. (Bryant, 1988; Bryant et al., 1988; Saito et al., 2002; Sobotkova et al., 1988; Zhong and Akkus, 2011). At physiological marrow temperature (35°C), intact bone marrow tissue has an effective Young's modulus range from 0.25-24.7 kPa (Table 9). Bovine bone marrow has a dynamic storage modulus of about 220 Pa at a frequency of 1.6 Hz and a temperature of 37 °C, according to the sole another study on the rheology of intact marrow (Winer et al., 2009). Our porcine samples had a dynamic storage modulus ranging from 23–10,000 Pa at this same frequency but at 35 °C (data not shown). Although their effort was limited to 3 samples from the same bone, this hindered their ability to detect biological heterogeneities in marrow samples. Nevertheless, this study is consistent with the storage magnitude we find for intact marrow. Because biological tissues are known to be diverse, it is not surprising that we discovered intact marrow to exhibit a significant level of inter-sample heterogeneity (Figure 3). For instance, reports on the elastic modulus of lung and brain tissue have been found to range from 1.5 to 100 kPa and 0.1 to 10 kPa, respectively (Booth et al., 2012; Chatelin et al., 2010; Lai-Fook and Hyatt, 2000; Melo et al., 2014; Miller et al., 2000; Rashid et al., 2013; Zhong and Akkus, 2011). It was crucial to confirm that the variety of mechanical tests employed to collect these data was not the source of this heterogeneity, as we have done here, even though it is more plausible that these variances are caused by structural elements of the tissues.

Preprints (www.preprints.org) | NOT PEER-REVIEWED | Posted: 27 December 2022 doi:10.20944/preprints202212.0503.v1

Table 9. Effective Young's Modulus comparisons for samples from the same bone using in vitro methods.

Marrow Sample Temperature	Rheology (kPa) 25°C	Indentation (kPa) 20°C	Cavitation (kPa) 20°C
1	52.1 ±10.2	30.3±4.0	64.3±0.2
2	4.0±0.9	5.7±0.3	9.0±0.01
3	0.7±0.3	0.9±0.2	0.9±0.2
4	3.2±1.9	2.1±0.3	14.4±10.0
5	84.4±6.5	35.3±4.9	no data
6	135.6±25.6	37.1±6.3	no data
7	69.0±21.4	—	—
8	—	12.2±2.8	—
9	—	—	16.0±1.6
Average	49.86	17.66	20.92

2. Results

Although there is a wide range of studies about FE Element analysis, there is not enough research to compare these analyses with different types of material properties (isotropic, anisotropic, and orthotropic). In this paper, important material properties for 3 sections of the bone (marrow, cortical, and trabeculae) were explained by reviewing the previous studies. One of the crucial tips in FE analysis of the femur is the lack of the model of the human femur with three mentioned sections and FE analysis of this model with different material properties. In this part, some similar research will be discussed to compare the impact of material properties on FE analysis on the femur.

Geraldes and Phillips compared orthotropic and isotropic bone adaptation in the femur (Geraldes and Phillips, 2014). They have done this research on the model of a human femur. It was a solid part, and they waived the trabeculae and marrow sections. The predicted forces and RMSE are shown in Tables 10 and 11.

Table 10. Hip contact forces' resulting components (Fr, Fx, Fy, and Fz) in (%BW) were predicted to have the following values for isotropic and orthotropic models.

Forces	Material	F_y	F_z	F_r
Predicted	Isotropic	59	−319	73
	Orthotropic	53	−306	71

Preprints (www.preprints.org) | NOT PEER-REVIEWED | Posted: 27 December 2022 doi:10.20944/preprints202212.0503.v1

Table 11. For the first third (0–33%), the last third (66–100%), and the entire width (0–100%) of the slice, the root mean squared error (RMSE,%) and Pearson's product-moment coefficient (r, p 0.0001) between the two distinct predictions (isotropic and orthotropic) and the CT scan profiles were calculated.

Slice	Region	Model	0–100%		0–33%		66–100%	
			RMSE (%)	*r*	RMSE (%)	*r*	RMSE (%)	*r*
1	5% femoral head	Iso	32.48	0.49	17.31	0.77	22.90	− 0.12
		Ortho	29.23	0.49	17.08	0.77	20.74	− 0.02
2	20% shaft	Iso	75.83	0.74	43.09	0.77	57.81	0.59
		Ortho	51.27	0.88	25.92	0.88	38.92	0.72
3	40% shaft	Iso	107.50	0.29	65.73	0.37	78.23	− 0.66
		Ortho	82.32	0.54	35.04	0.72	64.87	− 0.09
4	60% shaft	Iso	63.95	0.67	28.38	0.86	55.40	0.37
		Ortho	64.03	0.65	36.38	0.89	48.41	0.74
5	80% shaft	Iso	72.34	0.53	34.80	0.73	53.69	0.60
		Ortho	68.29	0.46	27.07	0.69	51.83	0.81
6	95% shaft	Iso	66.15	0.43	30.57	0.85	42.81	0.64
		Ortho	66.10	0.25	21.43	0.89	45.24	0.80
7	Neck	Iso	25.65	0.72	18.53	0.89	17.21	0.68
		Ortho	12.29	0.88	9.56	0.93	5.38	0.89
8	Greater trochanter	Iso	26.67	0.58	22.48	0.82	12.47	− 0.14
		Ortho	30.72	0.55	26.08	0.81	14.90	− 0.13
9	Femoral head	Iso	30.06	0.40	23.60	0.46	16.81	0.26
		Ortho	25.87	0.50	19.31	0.40	15.98	0.24
10	Femoral head	Iso	28.72	0.55	20.48	0.73	17.35	0.17
		Ortho	24.53	0.60	18.01	0.73	14.25	0.24
11	Femoral shaft	Iso	82.43	0.57	45.73	0.67	63.81	0.10
		Ortho	65.87	0.69	32.45	0.83	50.73	0.46
12	Femoral condyles	Iso	69.25	0.48	32.69	0.79	48.25	0.62
		Ortho	67.20	0.35	24.25	0.79	48.54	0.80
13	Whole femur	Iso	55.63	0.54	31.61	0.72	39.70	0.25
		Ortho	47.79	0.58	24.21	0.77	34.03	0.44

Anterior-posterior (A-P) bending load versus deflection curve with an approximative elastic bending stiffness of 318 N/mm is shown by Yamada (Yamada, 1970). A 364 N/mm elastic bending stiffness is reported by Mather (Mather, 1967). For example, the isotropic FE femur predicts 267 N/mm of bending stiffness, while the orthotropic and transversely isotropic femur models estimate 278 N/mm (Table 12).

Preprints (www.preprints.org) | NOT PEER-REVIEWED | Posted: 27 December 2022 doi:10.20944/preprints202212.0503.v1

Table 12. Result of Elastic Bending Stiffness.

Material properties	Elastic Bending Stiffness of the bone
Isotropic	267
Orthotropic	278
Anisotropic	278

When adopting the material model input moduli mentioned above, the transversely isotropic model and the orthotropic model's entire bone elastic stiffness are the same, and the isotropic model is 4% less stiff.

In order to compare the isotropic-piecewise-plasticity model utilized in this study with the 3-point A-P bending femur characteristics and test curves reported by Yamada (Yamada, 1970) and Mather (Mather, 1967), respectively. For each of the published research and the model, Table 13 lists the proportionate limit of deflection and the proportional load. Furthermore, Yamada (Yamada, 1970) indicates that the elastic modulus of the femur is 18.34 kN/mm² (based on the mid-diaphysis cross-sectional characteristics of the femur, the proportional limit deflection, and load) and the current investigation reveals a value of 18.0 kN/mm² that is similar.

Table 13. FE model comparison in published about whole-bone load against A-P deflection.

Load Curve	Range of Deflection in Proportion	Proportion Load
Yamada (Yamada, 1970)	6.0-7.0	2.10
Mather (Mather, 1967)	6.0-8.0	2.45
FE Model	8.0-9.0	2.50

The elastic limit "corresponds to around 50% of the ultimate torsion strength for the femur of any animal," according to Yamada (3). As a result, the analysis of the linear FE femur models is limited to values below 22.7 N/mm² or less than half of the ultimate torsion strength of 45.3 N/mm². The maximum twist angle is roughly 1.5°. According to Cristofolini et al. (Cristofolini et al., 1996), fresh-frozen femur samples have an elastic stiffness in the torsion range of 6.5-10.5 Nm/ deg. The isotropic FE femur model has a higher stiffness of 19.4 Nm/deg, and the orthotropic and transversely isotropic femur models show stiffness in torsion that is closer to the literature at 11.64 Nm/deg. Each FE femur model's elastic whole bone torsion stiffness is listed in Table 14. The transversely isotropic model and the orthotropic model have identical whole-bone elastic torsion stiffnesses, with the isotropic model having a 50% greater stiffness.

Table 14. Result of Elastic Torsion Stiffness.

Material properties	Elastic Torsion Stiffness of the bone
Isotropic	19.4
Orthotropic	11.6
Anisotropic	11.6

These findings support the idea that an isotropic material model of the human femur bone tissues, as opposed to a more intricate anisotropic model, is sufficient to predict whole bone bending response in the linear range. Particularly, the load versus deflection response of the isotropic model is closely followed by the orthotropic material model, which is equal to the transversely isotropic FE model. Additionally, as demonstrated in Figure 4, the nonlinear, isotropic model closely mimics the actual bone response, and the inclusion of fundamental nonlinearities in the material model (as accomplished here using a piecewise-linear material model) is crucial for strains greater than the linear range. The

 doi:10.20944/preprints202212.0503.v1

total bone reaction in torsion between the isotropic and anisotropic femur models, however, differs significantly. Due to the slight difference in shear moduli between the two anisotropic models, the two elicit whole bone responses that are once again identical. Shear modulus input is absent from the isotropic material model, which increases the primary stiffness in the calculations and results in a significantly stiffer structure under torsion. Anisotropic modeling is advised for these loading situations because the whole-bone torsion stiffness of the anisotropic material models is closer to the values indicated in the literature. The degree of anisotropy that should be included in the material model descriptions of the bone tissue constituents depends on the method of loading on the femur bone. The material models for the cortical and cancellous bone do not necessarily need to describe anisotropy if the entire bone is being loaded in bending. As a result, it is no longer necessary to gather data for and troubleshoot a more intricate FE model for bending tests. The isotropic FE femur model can be employed with adequate precision in place of the more complex models since it nearly approximates both the anisotropic FE femur models in bending. Due to the fewer material constants needed for the simpler material models, simplifying the FE model makes implementation simpler. Additionally, it makes model development and calculation more time-effective.

3. Conclusion

The findings of this analysis provide credence to the following assertions: 1- For material models of femur bone tissues in the elastic range of entire bone bending, material anisotropy is not required. 2- Simple non-linear, isotropic material models accurately mimic the bending behavior of actual bones. 3- The material model of the bone tissues must incorporate particular shear moduli in the plane of shear when the entire femur bone is being loaded in torsion. The findings of this analysis provide credence to the following assertions: 1- For material models of femur bone tissues in the elastic range of entire bone bending, material anisotropy is not required. 2- Simple non-linear, isotropic material models accurately mimic the bending behavior of actual bones. 3- The material model of the bone tissues must incorporate particular shear moduli in the plane of shear when the entire femur bone is being loaded in torsion.

Author Contributions: For research articles with several authors, a short paragraph specifying their individual contributions must be provided. The following statements should be used "Conceptualization, Andreas Baumgart; methodology, Holm Altenbatch.; software, Pourya Bazyar.; validation, Anna Usbeck., Andreas Baumgart; investigation, Holm Altenbatch.; resources, Pourya Bazyar.; data curation, Pourya Bazyar.; writing—original draft preparation, Pourya Bazyar.; writing—review and editing, Andreas Baumgart.; visualization, Andreas Baumgart.; supervision, Holm Altenbatch.; project administration, Holm Altenbatch. All authors have read and agreed to the published version of the manuscript." Please turn to the CRediT taxonomy for the term explanation. Authorship must be limited to those who have contributed substantially to the work reported.

Funding: Please add: "This research received no external funding. However, publication fee will be paid by Hamburg University of Applied science

Institutional Review Board Statement: Not applicable.

Informed Consent Statement: Not applicable.
Data Availability Statement: MDPI Research Data Policies" at https://www.mdpi.com/ethics.

Acknowledgments: We appreciate support of the authorities of Hamburg University of Applied science and Otto-von-Guericke-University Magdeburg.

Conflicts of Interest: The authors declare no conflict of interest.

References

1. Petrakis, N. L. (1952). Temperature of human bone marrow. Journal of Applied Physiology, 4(7), 549-553. https://doi.org/10.1152/jappl.1952.4.7.549.

2. Bryant, J. D., David, T., Gaskell, P. H., King, S., & Lond, G. (1989). Rheology of bovine bone marrow. Proceedings of the Institution of Mechanical Engineers, Part H: Journal of Engineering in Medicine, 203(2), 71-75. https://doi.org/10.1243/PIME_PROC_1989_203_013_01.
3. Geraldes, D. M., & Phillips, A. T. (2014). A comparative study of orthotropic and isotropic bone adaptation in the femur. International journal for numerical methods in biomedical engineering, 30(9), 873-889. https://doi.org/10.1002/cnm.2633.
4. Bryant, J. D. (1988). On the mechanical function of marrow in long bones. Engineering in medicine, 17(2), 55-58. https://doi.org/10.1243/EMED_JOUR_1988_017_017_02.
5. Lai-Fook, S. J., & Hyatt, R. E. (2000). Effects of age on elastic moduli of human lungs. Journal of applied physiology, 89(1), 163-168. https://doi.org/10.1152/jappl.2000.89.1.163.
6. Rashid, B., Destrade, M., & Gilchrist, M. D. (2013). Influence of preservation temperature on the measured mechanical properties of brain tissue. Journal of biomechanics, 46(7), 1276-1281. https://doi.org/10.1016/j.jbiomech.2013.02.014.
7. Melo, E., Cárdenes, N., Garreta, E., Luque, T., Rojas, M., Navajas, D., & Farré, R. (2014). Inhomogeneity of local stiffness in the extracellular matrix scaffold of fibrotic mouse lungs. Journal of the mechanical behavior of biomedical materials, 37, 186-195. https://doi.org/10.1016/j.jmbbm.2014.05.019.
8. Miller, K., Chinzei, K., Orssengo, G., & Bednarz, P. (2000). Mechanical properties of brain tissue in-vivo: experiment and computer simulation. Journal of biomechanics, 33(11), 1369-1376. https://doi.org/10.1016/S0021-9290(00)00120-2.
9. Booth, A. J., Hadley, R., Cornett, A. M., Dreffs, A. A., Matthes, S. A., Tsui, J. L., ... & White, E. S. (2012). Acellular normal and fibrotic human lung matrices as a culture system for in vitro investigation. American journal of respiratory and critical care medicine, 186(9), 866-876. https://doi.org/10.1164/rccm.201204-0754OC.
10. Chatelin, S., Constantinesco, A., & Willinger, R. (2010). Fifty years of brain tissue mechanical testing: from in vitro to in vivo investigations. Biorheology, 47(5-6), 255-276. DOI: 10.3233/BIR-2010-0576.
11. Winer, J. P., Janmey, P. A., McCormick, M. E., & Funaki, M. (2009). Bone marrow-derived human mesenchymal stem cells become quiescent on soft substrates but remain responsive to chemical or mechanical stimuli. Tissue Engineering Part A, 15(1), 147-154. https://doi.org/10.1089/ten.tea.2007.0388.
12. Saito, H., Lai, J., Rogers, R., & Doerschuk, C. M. (2002). Mechanical properties of rat bone marrow and circulating neutrophils and their responses to inflammatory mediators. Blood, The Journal of the American Society of Hematology, 99(6), 2207-2213. https://doi.org/10.1182/blood.V99.6.220
13. Sobotková, E., Hrubá, A., Kiefman, J., & Sobotka, Z. (1988). Rheological behaviour of bone marrow. In Progress and trends in rheology II (pp. 467-469). Steinkopff, Heidelberg. https://doi.org/10.1007/978-3-642-49337-9_165.
14. Zhong, Z., & Akkus, O. (2011). Effects of age and shear rate on the rheological properties of human yellow bone marrow. Biorheology, 48(2), 89-97. DOI: 10.3233/BIR-2011-0587.
15. Czarnecki, S. (2015). Isotropic material design. Computational Methods in Science and Technology, 21(2), 49-64. DOI:10.12921/cmst.2015.21.02.001.
16. M.J. Mirzaali, et al., Mechanical properties of cortical bone and their relationships with age, gender, composition and microindentation properties in the elderly, Bone (2016), http://dx.doi.org/10.1016/j.bone.2015.11.018.
17. Bazyar, P. & Baumgart, A. (2021). Effects of Additional Mechanisms on The Performance of Workshop Crane. Journal of Engineering in Industrial research, 3(2), 87-98. https://doi.org/10.22034/jeires.2022.2.1
18. Peng, L., Bai, J., Zeng, X., & Zhou, Y. (2006). Comparison of isotropic and orthotropic material property assignments on femoral finite element models under two loading conditions. Medical engineering & physics, 28(3), 227-233. https://doi.org/10.1016/j.medengphy.2005.06.003.

19. Bazyar, P., Jafari, A., Alimardani, R., Mohammadi, V., & Grichar, J. (2020). Finite Element Analysis of Small-scale Head of Combine Harvester for Harvesting Fine-Grain Products. International Journal of Advanced Biological and Biomedical Research, 8(4), 340-358. DOI: 10.33945/SAMI/IJABBR.2020.
20. Jacrot, B. (1976). The study of biological structures by neutron scattering from solution. Reports on progress in physics, 39(10), 911. DOI: 10.1088/0034-4885/39/10/001.
21. Amini, A. R., Laurencin, C. T., & Nukavarapu, S. P. (2012). Bone tissue engineering: recent advances and challenges. Critical Reviews™ in Biomedical Engineering, 40(5). DOI: 10.1615/CritRevBiomedEng.v40.i5.10.
22. MATHER, B. S. (1967). Correlations between strength and other properties of long bones. Journal of Trauma and Acute Care Surgery, 7(5), 633-638. doi: 10.1097/00005373-196709000-00003.
23. Yamada, H., & Evans, F. G. (1970). Strength of biological materials. https://scholar.google.com/scholar?hl=en&as_sdt=0%2C5&q=Yamada%2C+H.%2C+%26+Evans%2C+F.+G.+%281970%29.+Strength+of+biological+materials.&btnG=.
24. Martens, M., Van Audekercke, R., De Meester, P., & Mulier, J. C. (1986). Mechanical behaviour of femoral bones in bending loading. Journal of Biomechanics, 19(6), 443-454. https://doi.org/10.1016/0021-9290(86)90021-7.
25. Keller, T. S., Mao, Z., & Spengler, D. M. (1990). Young's modulus, bending strength, and tissue physical properties of human compact bone. Journal of orthopaedic research, 8(4), 592-603. https://doi.org/10.1002/jor.1100080416.
26. Zani, L., Erani, P., Grassi, L., Taddei, F., & Cristofolini, L. (2015). Strain distribution in the proximal Human femur during in vitro simulated sideways fall. Journal of Biomechanics, 48(10), 2130-2143. https://doi.org/10.1016/j.jbiomech.2015.02.022.
27. Arun, K. V., & Jadhav, K. K. (2016). Behaviour of human femur bone under bending and impact loads. Eur. J. Clin. Biomed. Sci, 2(6). DOI: 10.11648/j.ejcbs.20160202.11.
28. Schuster, P., & Jayaraman, G. (2000). Development and validation of a pedestrian lower limb non-linear 3-D finite element model. Stapp car crash journal, 44, 315. URL: https://digitalcommons.calpoly.edu/meng_fac/118.
29. Pellettiere, J. A. (1999). A dynamic material model for bone. University of Virginia. URL: https://www.proquest.com/openview/4b2efe43d488716177b54e8027c35af6/1?pq-origsite=gscholar&cbl=18750&diss=y
30. Wirtz, D. C., Schiffers, N., Pandorf, T., Radermacher, K., Weichert, D., & Forst, R. (2000). Critical evaluation of known bone material properties to realize anisotropic FE-simulation of the proximal femur. Journal of biomechanics, 33(10), 1325-1330. https://doi.org/10.1016/S0021-9290(00)00069-5.
31. Ciarelli, M. J., Goldstein, S. A., Kuhn, J. L., Cody, D. D., & Brown, M. B. (1991). Evaluation of orthogonal mechanical properties and density of human trabecular bone from the major metaphyseal regions with materials testing and computed tomography. Journal of Orthopaedic Research, 9(5), 674-682. https://doi.org/10.1002/jor.1100090507.
32. Cristofolini, L., Viceconti, M., Cappello, A., & Toni, A. (1996). Mechanical validation of whole bone composite femur models. Journal of biomechanics, 29(4), 525-535. https://doi.org/10.1016/0021-9290(95)00084-4.
33. Osterhoff, G., Morgan, E. F., Shefelbine, S. J., Karim, L., McNamara, L. M., & Augat, P. (2016). Bone mechanical properties and changes with osteoporosis. Injury, 47, S11-S20. https://doi.org/10.1016/S0020-1383(16)47003-8.
34. Reilly, D. T., & Burstein, A. H. (1974). The mechanical properties of cortical bone. JBJS, 56(5), 1001-1022. URL: https://journals.lww.com/jbjsjournal/Citation/1974/56050/The_Mechanical_Properties_of_Cortical_Bone.12.aspx
35. Choi, K., Kuhn, J. L., Ciarelli, M. J., & Goldstein, S. A. (1990). The elastic moduli of human subchondral, trabecular, and cortical bone tissue and the size-dependency of cortical bone modulus. Journal of biomechanics, 23(11), 1103-1113. https://doi.org/10.1016/0021-9290(90)90003-L.

36. Ciarelli, M. J., Goldstein, S. A., Kuhn, J. L., Cody, D. D., & Brown, M. B. (1991). Evaluation of orthogonal mechanical properties and density of human trabecular bone from the major metaphyseal regions with materials testing and computed tomography. Journal of Orthopaedic Research, 9(5), 674-682. https://doi.org/10.1002/jor.1100090507.
37. Keaveny, T. M., Guo, X. E., Wachtel, E. F., McMahon, T. A., & Hayes, W. C. (1994). Trabecular bone exhibits fully linear elastic behavior and yields at low strains. Journal of biomechanics, 27(9), 1127-1136. https://doi.org/10.1016/0021-9290(94)90053-1.
38. Bayraktar, H. H., Morgan, E. F., Niebur, G. L., Morris, G. E., Wong, E. K., & Keaveny, T. M. (2004). Comparison of the elastic and yield properties of human femoral trabecular and cortical bone tissue. Journal of biomechanics, 37(1), 27-35. https://doi.org/10.1016/S0021-9290(03)00257-4.
39. Augat, P., Link, T., Lang, T. F., Lin, J. C., Majumdar, S., & Genant, H. K. (1998). Anisotropy of the elastic modulus of trabecular bone specimens from different anatomical locations. Medical engineering & physics, 20(2), 124-131. https://doi.org/10.1016/S1350-4533(98)00001-0.
40. Zysset, P. K. (2003). A review of morphology–elasticity relationships in human trabecular bone: theories and experiments. Journal of biomechanics, 36(10), 1469-1485. https://doi.org/10.1016/S0021-9290(03)00128-3.
41. Kabel, J., van Rietbergen, B., Dalstra, M., Odgaard, A., & Huiskes, R. (1999). The role of an effective isotropic tissue modulus in the elastic properties of cancellous bone. Journal of biomechanics, 32(7), 673-680. https://doi.org/10.1016/S0021-9290(99)00045-7.
42. Morgan, E. F., Bayraktar, H. H., & Keaveny, T. M. (2003). Trabecular bone modulus–density relationships depend on anatomic site. Journal of biomechanics, 36(7), 897-904. https://doi.org/10.1016/S0021-9290(03)00071-X.
43. Morgan, E. F., & Keaveny, T. M. (2001). Dependence of yield strain of human trabecular bone on anatomic site. Journal of biomechanics, 34(5), 569-577. https://doi.org/10.1016/S0021-9290(01)00011-2.
44. Falcinelli, C., & Whyne, C. (2020). Image-based finite-element modeling of the human femur. Computer Methods in Biomechanics and Biomedical Engineering, 23(14), 1138-1161. https://doi.org/10.1080/10255842.2020.1789863.
45. Chethan, K. N., Zuber, M., & Shenoy, S. (2019). Finite element analysis of different hip implant designs along with femur under static loading conditions. Journal of Biomedical Physics & Engineering, 9(5), 507. DOI: 10.31661/jbpe.v0i0.1210.
46. Schileo, E., Pitocchi, J., Falcinelli, C., & Taddei, F. (2020). Cortical bone mapping improves finite element strain prediction accuracy at the proximal femur. *Bone*, *136*, 115348. https://doi.org/10.1016/j.bone.2020.115348.
47. Zhang, Y., Li, A. A., Liu, J. M., Tong, W. L., Xiao, S. N., & Liu, Z. L. (2022). Effect of screw tunnels on proximal femur strength after screw removal: A finite element analysis. Orthopaedics & Traumatology: Surgery & Research, 108(8), 103408. https://doi.org/10.1016/j.otsr.2022.103408.
48. Tucker, S. M., Wee, H., Fox, E., Reid, J. S., & Lewis, G. S. (2019). Parametric finite element analysis of intramedullary nail fixation of proximal femur fractures. Journal of Orthopaedic Research®, 37(11), 2358-2366. https://doi.org/10.1002/jor.24401.
49. Mobasseri, S., Karami, B., Sadeghi, M., & Tounsi, A. (2022). Bending and torsional rigidities of defected femur bone using finite element method. Biomedical Engineering Advances, 3, 100028. https://doi.org/10.1016/j.bea.2022.100028.
50. Kalaiyarasan, A., Sankar, K., & Sundaram, S. (2020). Finite element analysis and modeling of fractured femur bone. Materials Today: Proceedings, 22, 649-653. https://doi.org/10.1016/j.matpr.2019.09.036.
51. Yeni, Y. N., Brown, C. U., Wang, Z., & Norman, T. L. (1997). The influence of bone morphology on fracture toughness of the human femur and tibia. Bone, 21(5), 453-459. DOI: 10.1016/s8756-3282(97)00173-7. https://doi.org/10.1016/S8756-3282(97)00173-7.

 doi:10.20944/preprints202212.0503.v1

52. Bazyar, P., Baumgart, A., Altenbatch, H., & Usbeck, A. (2022). Optimization of a simplified model of the human femur with inner structure and real material properties. DOI: 10.21203/rs.3.rs-2377594/v1.
53. Ahn, S. H., Montero, M., Odell, D., Roundy, S., & Wright, P. K. (2002). Anisotropic material properties of fused deposition modeling ABS. Rapid prototyping journal. URL: https://www.emerald.com/insight/content/doi/10.1108/13552540210441166/full/html?casa_token=NZHMQUutX98AAAAA:hAYM9lDkITmpgApyvA6h8q_71p3ZWU2WNHJ1ZehYC_IHR3Ugx2JUj_PFYK9gqCBQH6lPnW9inX6ALxehn6Op3vTzuR0KHOpDbMX0JAj1zv2oWZy_.
54. Katsamanis, F., & Raftopoulos, D. D. (1990). Determination of mechanical properties of human femoral cortical bone by the Hopkinson bar stress technique. Journal of biomechanics, 23(11), 1173-1184. https://doi.org/10.1016/0021-9290(90)90010-Z.